Materials Transactions, Vol. 60, No. 2 (2019) pp. 263 to 268

Quantitative Analysis on Light Elements Solution Strengthening in Pure Titanium Sintered Materials by Labusch Model Using Experimental Data*1

Shota Kariya[1,2,*2], Mizuki Fukuo[1,*2], Junko Umeda[2] and Katsuyoshi Kondoh[2,*3]

[1]*Department of Mechanical Engineering, Graduate School of Osaka University, Suita 565-0871, Japan*
[2]*Joining and Welding Research Institute, Osaka University, Ibaraki 567-0047, Japan*

Solid solution strengthening effect by oxygen (O) and nitrogen (N) atoms of α-titanium (Ti) materials was quantitatively evaluated using Labusch model by consideration of the experimental data. When using Labusch model to predict solid solution strengthening improvement, an application of the isotropic strains by solute elements is generally assumed to estimate Fm value. It is, however, difficult to exactly calculate Fm value for α-Ti materials with O and N solute atoms because the anisotropic strains are induced in α-Ti crystal with hcp structure by these elements. In this study, Fm value was experimentally derived from the relationship between 0.2% yield stress and solute elements (O and N atoms) content of powder metallurgy Ti materials. As a result, the strengthening improvement was proportional to $c^{2/3}/S_f$ (c: soluted atom content, S_f: Schmid factor), and its factor of proportionality of Ti–O and Ti–N materials was 4.17×10^3 and 3.29×10^3, respectively. According to this analysis, it was clarified that Fm value of Ti–O and Ti–N materials was 6.22×10^{-10} and 5.21×10^{-10}, respectively, and then the estimated strengthening improvement by using these values was significantly agreed with the experimental results of PM Ti materials with O and N solution atoms. [doi:10.2320/matertrans.Y-M2018849]

(Received September 11, 2018; Accepted October 19, 2018; Published January 25, 2019)

Keywords: *solid solution, titanium, oxygen, nitrogen, Labusch model*

1. Introduction

Titanium (Ti) has excellent properties such as high specific strength, excellent corrosion resistance and high biocompatibility due to the osseointegration.[1,2] These performances make it possible to apply Ti materials to the medical devices and transport instruments.[3–7] From a viewpoint of the strength improvement, there is a serious problem of the conventional Ti–6 Al–4 V alloy (ASTM B348 Gr5) because it contains vanadium element which is one of toxic and expensive rare metals.[8] Regarding this issue, recently the ubiquitous element such as oxygen, nitrogen, carbon, silicon, iron etc., are employed instead of rare metals used as the alloying elements to improve the mechanical strength of Ti materials. For instance, there are Ti materials strengthened by TiC particles produced via a reaction between additional carbon particles and titanium matrix,[9,10] grains refinement using silicon addition,[11,12] and solid solution using oxygen or nitrogen atoms.[13–18] In these materials, Orowan mechanism and Hall-Petch relationship are often used to quantitatively estimate the effect of ubiquitous element addition on the increment of their yield strength.[19–21] Furthermore, in regard to estimation of solid solution strengthening in metals, Cottrell proposed the model regarding the pinning effect on dislocations movement by solute atoms,[22] and Fleischer and Friedel explained the role of obstacles touched by dislocations under the stress applied.[23,24] However, no consideration on the interaction between the solute atoms was taken in these models. Mott, Nabarro and others established many theories which overcome this problem,[25] and many researchers previously employed these models to quantitatively understand and calculate the solid solution strengthening effect. Labusch also established the similar model regarding the solid solution strengthening behavior.[26] In this model, the strengthening increment was predicted by using the premises that solute atoms apply isotropic strain. Therefore, it is difficult to apply Labusch model on α-Ti material having an anisotropic strain due to its hcp structure.[27] At this moment, there is no report to show a good agreement between experimental data and calculated results by using above-mentioned models regarding the interstitial solid solution strengthening of α-Ti materials.

This study discussed the effect of the interstitial solid solution elements such as oxygen and nitrogen on the microstructures and mechanical properties of powder metallurgy (PM) Ti materials with oxygen or nitrogen atoms. In particular, the parameters used in Labusch model was obtained from the experimental data, and the solid solution strengthening increment of PM Ti–O and Ti–N materials was quantitatively calculated. As a result, a good agreement between experimental data and calculated results was obtained.

2. Experimental Procedure

2.1 Materials fabrication

Commercial pure Ti powder (TC-450, TOHO TECHNICAL SERVICE Co., Ltd) and TiO_2 particles (KOJUNDO CHEMICAl LABORATORY Co., Ltd) were used as starting materials. Pure Ti powder prepared by the hydride and dehydride (HDH) process, having a mean particle size of 27.8 µm, shows a typical irregular morphology. TiO_2 particles with around 3.6 µm mean particle size were employed as oxygen providers to pure Ti materials. In this experiment, each elemental mixture (200 g) of pure Ti and TiO_2 powder such as Ti–0.5 mass% TiO_2, Ti–1.0 mass% TiO_2, Ti–1.5 mass% TiO_2 and Ti–2.0 mass% TiO_2, was put into the jar, and uniformly mixed by rock milling process (60 Hz, 3.6 ks).

*1This Paper was Originally Published in Japanese in J. Jpn. Soc. Powder Powder Metallurgy **65** (2018) 407–413.
*2Graduate Student, Osaka University
*3Corresponding author, E-mail: kondoh@jwri.osaka-u.ac.jp

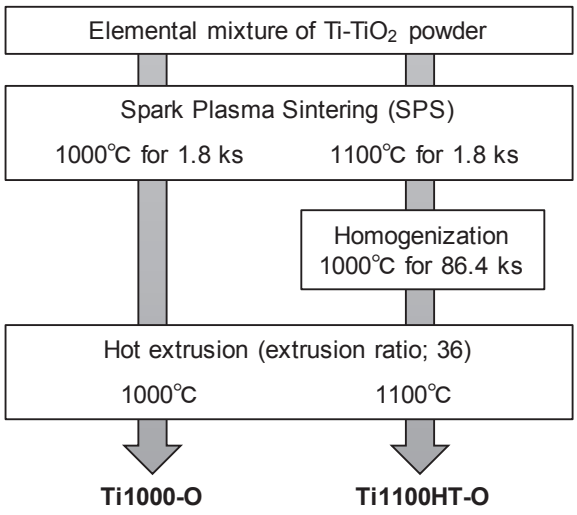

Fig. 1 Flowchart of specimen preparation of Ti1000-O and Ti1100HT-O materials by powder metallurgy route.

The powder mixture was consolidated using a spark plasma sintering (SPS, SPS-1030, SPS Syntex Inc.). The SPS conditions at 1000 and 1100°C for 1.8 ks in vacuum (6 Pa) were selected, and 30 MPa pressure was applied to the powder in the carbon die. The diameter of each SPSed columned billet was 42 mm.

The homogenization heat treatment at 1000°C for 86.4 ks was applied to the latter billet by using the vacuum furnace (FT-1200R-120, FULL-TECH FURNACE Co., Ltd). The SPSed billets were extruded by a hydraulic direct press machine (SHP-200-450, Shibayama kikai Co., Ltd), where the extrusion speed was 3 mm s^{-1}, the extrusion die diameter was 7 mm and the extrusion ratio was 36. Before hot extrusion, the billet was pre-heated at 1000 and 1100°C for 300 s in Ar gas atmosphere using the image furnace, and immediately supplied to the extrusion process. Each extruded rod was named as Ti1000-O and Ti1100HT-O, respectively as shown in Fig. 1.

2.2 Materials characterization

Oxygen (O) and nitrogen (N) contents of the extruded rods were measured using a highly accurate O/N/H analyzer (EMGA-930, HORIBA, Ltd.). The microstructures of final products were characterized using X-ray diffraction (XRD, XRD-6100, SHIMADZU Corp.) and electron back-scatter diffraction (EBSD) that attached to a field emission scanning electron microscopy (FE-SEM, JSM-6500F, JEOL Ltd.). EBSD samples were polished by electro-chemical etching using 95 vol% CH_3COOH + 5 vol% $HClO_4$ solution with 20 V for 60∼90 s. The tensile properties of these samples were evaluated at room temperature under a nominal strain rate of 5.0×10^{-4}/s using a mechanical tensting machine (Autograph AG-X 50 kN, SHIMADZU CORPORATION). At least two tensile specimens with 15 mm in gauge length and 3 mm in diameter were machined from each extruded rod.

3. Results and Discussion

In order to investigate the solid solution strengthening effect by oxygen and nitrogen elements on the mechanical properties of PM titanium materials, each content of Ti1000-O and Ti1100HT-O samples was analyzed. Oxygen and nitrogen contents of raw pure Ti powder, Ti1000-O and Ti1100HT-O materials were shown in Table 1, where the calculated oxygen content from TiO_2 addition was also shown. Nitrogen content of each material was 0.07 at%, that is, there was no significant difference in all samples. On the other hand, the oxygen content of each material gradually increased with increase in the TiO_2 addition, and agreed well with the calculated value as shown in Table 1. It means that the oxygen content of the extruded materials can be quantitatively controlled by TiO_2 particle addition. Ti material with 2 mass% TiO_2 addition (Ti1100HT-2.76O) has an extremely high oxygen content of 2.76 at% compared with ASTM/ASME Grade 1 (0.54 at%) and Grade 4 (1.19 at%) pure Ti.

XRD analysis on Ti1000-O and Ti1100HT-O was conducted in order to evaluate the solid solution behavior

Table 1 Oxygen and nitrogen contents of raw pure Ti powder and PM Ti–O materials in this study, and calculated oxygen content from TiO_2 addition of each material.

	Oxygen content (at.%)	Nitrogen content (at.%)	Calculated oxygen content (at.%)
Pure Ti powder	0.62	0.07	0.62 (Base)
Ti1000-0.65O	0.65	0.07	0.62 (Base)
Ti1000-1.35O	1.35	0.07	1.21
Ti1000-1.76O	1.76	0.07	1.80
Ti1000-2.34O	2.34	0.07	2.38
Ti1100HT-0.60O	0.60	0.07	0.62 (Base)
Ti1100HT-1.68O	1.68	0.07	1.80
Ti1100HT-2.76O	2.76	0.07	2.96

in α-Ti crystal with a hexagonal close packing (hcp) structure. It is well known that α-Ti crystal lattice is expanded in c-axis direction by the interstitial solid solution elements such as oxygen and nitrogen atoms.[27] Figure 2 indicates XRD analysis results of Ti1100HT-O with various oxygen contents. In this study, each XRD profile shows no peak shift at 74.04° corresponding to (200) cylindrical plane which is not affected by the lattice expansion behavior in c-axis direction. On the other hand, α-Ti peaks at 70.66°, 76.22° and 77.55° related to basal and prismatic planes obviously shifted to a lower angle due to the interstitial solid-solution phenomenon. By using the XRD peak shifts shown in Fig. 2 and that of Ti1000-O, the dependence of the lattice parameters of α-Ti hcp structure in a-axis and c-axis directions on the oxygen content were calculated. As shown in Fig. 3, the lattice constant in c-axis direction (b) proportionally increased with increase in oxygen contents while that in a-axis (a) revealed no change in increasing the oxygen content. Previous studies reported that the TiO_2 particles were thermally decomposed during sintering with Ti powder.[13,14,28] In this study, too, oxygen atoms should be in solid solution, because we applied higher temperature and longer time in the heat treatment to the SPSed billets. Therefore, the additive TiO_2 particles were completely decomposed and all oxygen atoms originated from TiO_2 particles were soluted into α-Ti crystals of Ti1100HT-O and Ti1000-O materials. It resulted in the lattice expansion in c-axis direction.

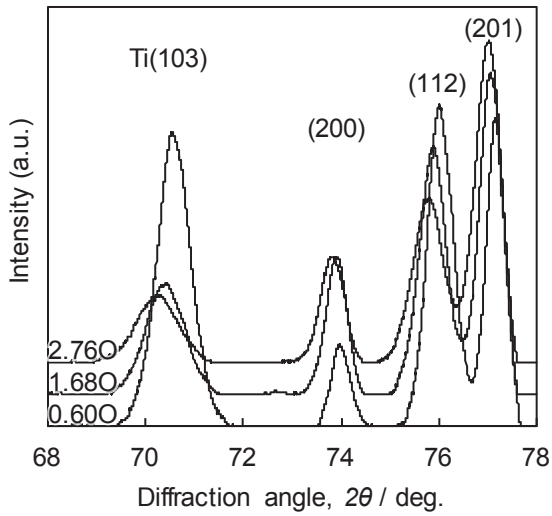

Fig. 2 XRD profiles of Ti1100HT-O materials with different oxygen contents.

IPF maps and inverse pole figures of Ti1100HT-O materials with oxygen content of 0.60 at%, 1.68 at% and 2.76 at% are shown in Fig. 4. The matrix of all samples consisted of equiaxial α-Ti grains, not acicular grains. The cooling rate after extrusion was about 6°C/s, and was enough to prevent the formation of martensite phases due to the transformation from β to α-Ti,[29] and resulted in the formation of equiaxial α-Ti grains in the extruded materials.

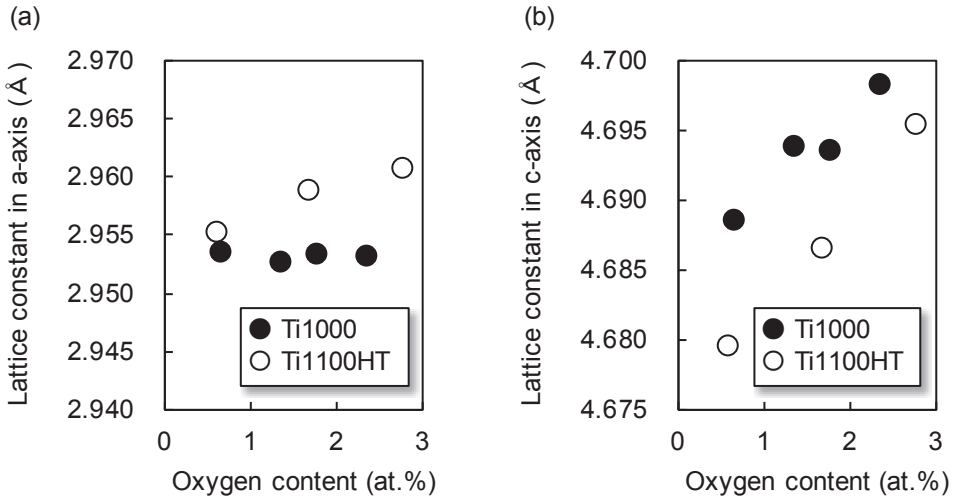

Fig. 3 Dependence of lattice parameters in (a) a-axis and (b) c-axis on oxygen content of Ti1000-O and Ti1100HT-O materials.

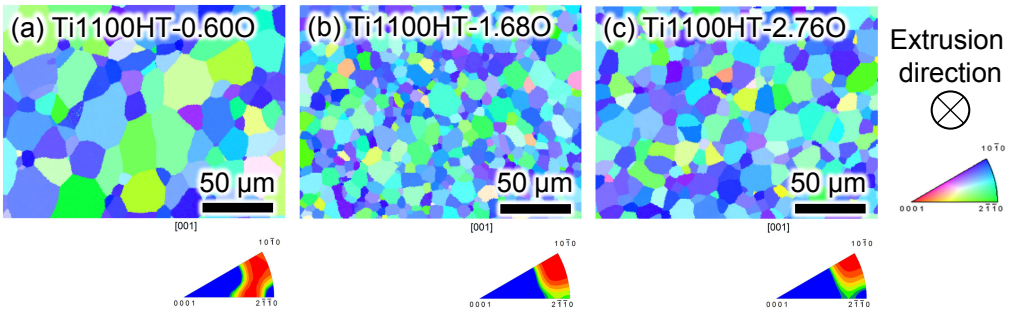

Fig. 4 IPF maps of Ti1100HT-O materials with (a) 0.60 at%, (b) 1.68 at% and (c) 2.76 at% oxygen.

Table 2 Mean grain size and Schmid's factor measurements of Ti1000-O and Ti1100HT-O materials.

	Grain size (μm)	Schmid's factor
Ti1000-0.65O	11.6	0.455
Ti1000-1.35O	9.3	0.454
Ti1000-1.76O	8.2	0.443
Ti1000-2.34O	8.7	0.459
Ti1100HT-0.60O	26.1	0.436
Ti1100HT-1.68O	11.3	0.455
Ti1100HT-2.76O	13.6	0.447

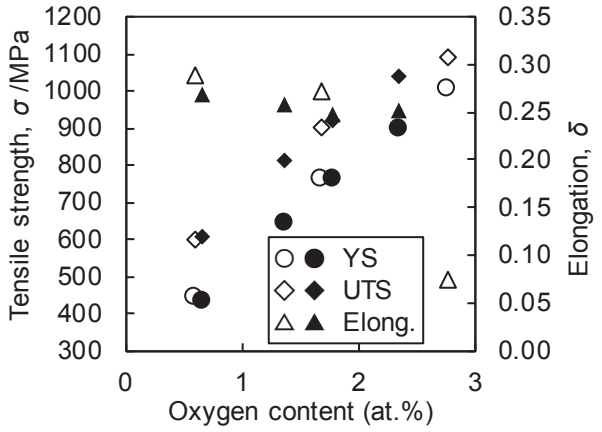

Fig. 5 Tensile properties dependence on oxygen content of Ti1000-O (closed) and Ti1100HT-O materials (opened).

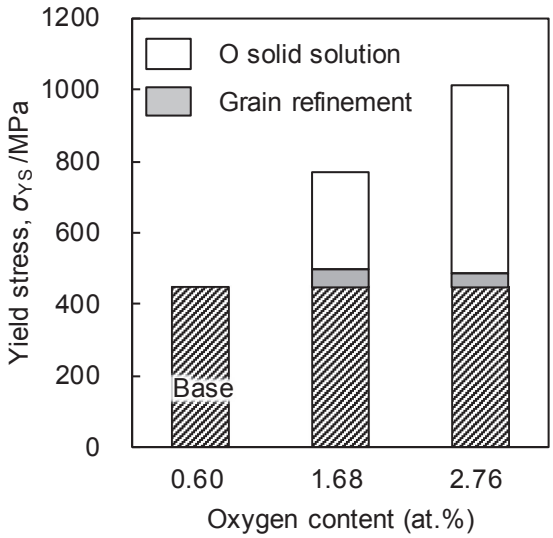

Fig. 6 Strengthening factors contribution to yield stress of Ti1100HT-O materials.

All specimens showed strong (10-10) cylindrical textures along the extrusion direction, that is, these texture formation was not related to the oxygen content of Ti1100HT-O materials. Table 2 shows the mean α-Ti grain size and Schmid factor of PM Ti materials prepared in this study. Ti1000-O materials had finer grains compared to Ti1100HT-O materials. This result is interpreted that the higher temperature SPS and heat treatment β phase which were applied to Ti1100HT-O materials resulted in the significant grain coarsening. In all specimens, the oxygen content increment caused α-Ti grains refinement because of the solute drag effect by agglomeration of oxygen soluted atoms at α-Ti grain boundaries.[30–32] For example, the grain size decreased from 11.6 μm to 8.2 μm in case of Ti1000-O and from 26.1 μm to 11.3 μm in Ti1100HT-O materials. It is obvious that a small amount of oxygen solution was effective to accelerate the grains refinement. When more than about 1 at% oxygen was soluted in the materials, however, the grain size was constant and never drastically changed because so much oxygen atoms existed at the boundaries and then the above mentioned solute drag effect was saturated. On the other hand, Schmid factor was 0.443∼0.459 and 0.436∼0.455 in Ti1000-O and Ti1100HT-O, respectively. In both materials, this factor was independent of the oxygen content. In general, Schmid factor is affected by the crystal structure and plastic working conditions.[33] As shown in Fig. 3(b), however, the oxygen solution in α-Ti grains of these specimens caused the lattice constant change from 4.680 Å to 4.695 Å in c-axis direction, that is, the expansion ratio was only 0.3%. Therefore, the lattice expansion by oxygen solution had very few effects on Schmid factor changes of PM extruded Ti materials, and the extrusion process strongly influenced Schmid factor of each specimen. In general, it is reported that crystal grains induced with plastic strain has multi-color or different shades.[34–36] However, IPF maps of extruded Ti1100HT materials with various oxygen contents showed the grains with unicolor. It means that the introduced strains in the matrix during hot extrusion was relieved due to dynamic recrystallization.

Figure 5 indicates tensile properties of Ti1000-O and Ti1100HT-O materials. 0.2% yield stress (0.2% YS) and ultimate tensile stress (UTS) increased with increase in the oxygen addition. The 0.2% YS and UTS were 445 and 602 MPa of Ti1100HT-0.60O, 765 and 903 MPa of Ti1100HT-1.68O and 1007 and 1094 MPa of Ti1100HT-2.76O, respectively. On the other hand, the elongation to failure was more than 20% when oxygen content was less than 2.34 at%. while it was 7.5% in case of oxygen content over 2.76 at%. The principal slip plane of hcp metals strongly depends on c/a ratio, where a basal plane slipping is dominant in long hcp structure (c/a > 1.61) and a prismatic plane slipping occurs in short hcp one (c/a < 1.61).[37] In addition, it is also reported that α-Ti materials with oxygen solid solution show poor ductility because the principal slip system changes from a prismatic plane to basal plane slipping due to the lattice expansion in c-axis direction by oxygen atoms solution. The strengthening contribution factors on 0.2% YS of Ti1100HT-O materials with different oxygen contents were shown in Fig. 6. As mentioned above, since TiO_2 particles were completely dissolved and there was no residual strain in EBSD analysis results, Therefore, it was deduced that there are neither effects of TiO_2 particles dispersion nor effects of residual strain on 0.2% YS increment. The major strengthening factors in Ti–O materials were both the grain refinement and the oxygen solid solution.

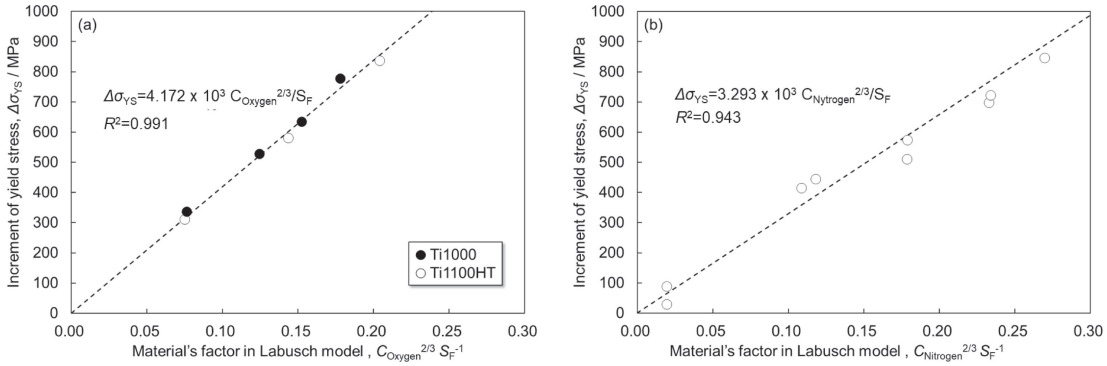

Fig. 7 Relationship between increment of yield stress by (a) oxygen and (b) nitrogen solid solution strengthening effects and material's factor in Labusch model.

Therefore, the oxygen solid solution strengthening factor could be considered quantitatively after modifying the grain refinement effect by Hall-Petch relationship. Hall-Petch constant of 15.7 MPa/mm^2 was used.[20] 0.2% YS increment by grain refinement from Ti1100HT-0.60O to Ti1100HT-1.68O and Ti1100HT-2.76O was 50 MPa and 37 MPa, respectively. These values were significantly small compared to oxygen solution strengthening of 269 MPa (Ti1100HT-1.68O) and 525 MPa (Ti1100HT-O-2.76O). It was concluded that the solid solution strengthening by oxygen atoms in α-Ti was the main factor to improve the mechanical strength of Ti–O materials.

In order to theoretically study the oxygen solution strengthening behavior of PM Ti–O materials, the quantitative evaluation of its strengthening effect by using Labusch model[26] dealing with the interaction between edge dislocations and solid solution atoms. In this model, the elastic interaction energy E is given by eq. (1), where Δ is a volume of solid solution atoms and the stress field σ in solute atom is considered to be a constant on the basis of hypothesis that distance between dislocation and solid solute atom is negligibly small compared with radius of solid solute atoms.

$$E = -\Delta\sigma_{ij}\varepsilon_{ij}. \tag{1}$$

When the solution atoms give isotropic stress, ε_{ij} is equal to $\varepsilon\ \delta_{ij}$. δ_{ij} corresponds to Kronecker's delta,[38] and then δ_{11}, δ_{22} and δ_{33} should be 1 and other components are 0. Therefore, eq. (1) could be expressed as the below eq. (2);

$$\begin{aligned} E &= -\Delta(\sigma_{11}\varepsilon_{11} + \sigma_{22}\varepsilon_{22} + \sigma_{33}\varepsilon_{33}) \\ &= -\Delta(\sigma_{11} + \sigma_{22} + \sigma_{33})\varepsilon. \end{aligned} \tag{2}$$

Expanding eq. (2) into eq. (3) under the conditions of edge dislocation, the elastic interaction energy about edge dislocation is shown as follows;

$$E = -\Delta Gb\frac{(1+\nu)}{3\pi(1-\nu)}\frac{y}{(x^2+y^2)} \tag{3}$$

where G is stiffness, b is size of burger's vector, ν is Poisson coefficient, and (x, y) is relative coordinates of the solid solute atom from an edge dislocation. Partial differentiating eq. (3) by a valuable x, the interaction force F (eq. (4)) between a solid solute atom and edge dislocation is obtainable.

$$F = \frac{\partial E}{\partial x} = \Delta Gb\frac{(1+\nu)}{3\pi(1-\nu)}\frac{2xy}{(x^2+y^2)^2}. \tag{4}$$

In Labusch model, the increment of 0.2% YS $\Delta\sigma_{YS}$ is shown in the below equation with F_m representing the maximum value of F,

$$\Delta\sigma_{YS} = \frac{\tau}{S_F} = \frac{c^{2/3}}{S_F}\left(\frac{{F_m}^4 w}{4Gb^9}\right)^{1/3} \tag{5}$$

where c is atomic ration of interstitial solid solute atom, S_F is Schmid factor, and w is parameter representing the area affected by interaction between an edge dislocation and solid solute atom. $({F_m}^4 w/4Gb^9)^{1/3}$ is constant on Ti–O material, and $c^{2/3}/S_F$ is various on oxygen content and fabrication process. However, solid solute oxygen atom applies anisotropic stress and strain on titanium crystal. Therefore, it is not possible to determine the parameter, F_m theoretically. In this study, hence, we derived this parameter experimentally from the tensile-test data as follows. In Fig. 7(a), 0.2% YS increment by the solid solution oxygen atom was plotted against the material's factor, $(c^{2/3}/S_F)$. We can determine this factor experimentally. It is obvious that a linear relationship was obtained as shown in Fig. 7(a). Here, it is noted that the straight line should pass the zero point. From the linear relationship, it was derived that the constant, $({F_m}^4 w/4Gb^9)^{1/3}$ of Ti–O materials is 4.17×10^3 and the parameter, F_m is 6.22×10^{-10}.

It is also reported that nitrogen atoms have a solid solution strengthening effect in α-Ti materials in similar to oxygen atoms.[27] In Fig. 7(b), 0.2% YS increment was plotted against the factor, $c^{2/3}/S_F$ in Ti–N materials. We employed the experimental data in previous study.[16] It is obvious that 0.2% YS increment again increased in proportion to the material's factor, $c^{2/3}/S_F$ ($R^2 = 0.943$). It was derived that the constant, $({F_m}^4 w/4Gb^9)^{1/3}$ of Ti–N materials is 3.29×10^3 and the parameter, F_m is 5.21×10^{-10}.

In order to evaluate the adequacy of the above F_m values of Ti–O and Ti–N materials, the calculated 0.2%YS increment of three kinds of Ti–O–N materials (Ti1100HT-0.97O-0.78N, Ti1100HT-1.25O-0.53N, Ti1100HT-1.54O-0.30N) by using Fm value was compared with the experimental value. The results are summarized in Table 3. Each Ti–O–N material was fabricated by using the pre-mixed Ti–TiO_2–TiN powders. Experimental data of 0.2% YS was 800 MPa for Ti1100HT-0.97O-0.78N, 789 MPa for Ti1100HT-1.25O-0.53N and 795 MPa for Ti1100HT-1.54O-0.30N, respectively. Each calculated 0.2%YS was modified by excluding the grains refinement strengthening effect. In Labusch model,

Table 3 Calculated solid solution strengthening effect and 0.2% YS increment modified from tensile test results.

(MPa)	① $\Delta\sigma_{YS}$[O]	② $\Delta\sigma_{YS}$[N]	① + ②	Modified 0.2% YS increment
Ti1100HT-0.97O-0.78N	97.8	206.4	304.2	306.0
Ti1100HT-1.25O-0.53N	179.3	140.1	319.4	299.7
Ti1100HT-1.54O-0.30N	254.6	69.9	324.5	317.0

the total increment of 0.2%YS of Ti–O–N materials was a sum of the increment by each solution atom because the interaction between a solid solute atom and dislocation was subscribed as an integrated value. As shown in Table 3, the calculated values of Ti–O–N materials by using Labusch model showed a good agreement with the experimental data. It is concluded that the solid solution strengthening of Ti–O and Ti–N materials can be successfully and quantitatively estimated by Labusch model with a suitable F_m value obtained by the experimental method proposed in this study.

4. Conclusion

It is difficult to calculate 0.2% YS increment by oxygen or nitrogen solid solution theoretically by Labusch model, since solid solution of oxygen applies anisotropic strain on α-Ti materials having a hcp structure. In this study, thereby, 0.2% YS increment by oxygen or nitrogen solid solution in the α-Ti materials was successfully calculated by the following procedures. At first, material's factor, $c^{2/3}/S_F$ was plotted against 0.2% YS increment by assuming the parameter, $(F_m{}^4 w/4Gb^9)^{1/3}$ is a constant. It was shown that linear relationship is obtainable between the 0.2% YS increment and the material's parameter both in Ti–O and Ti–N materials. Then, the proportion coefficient and hence the maximum force (F_m) between the edge dislocation and solid solution atom was determined from such a linear relationship. F_m was 6.22×10^{-10} for Ti–O materials and 5.21×10^{-10} for Ti–N materials. Finally, the present model was applied to Ti–O–N materials. It was concluded that the calculated 0.2% YS increment shows a good agreement with the experimental results.

Acknowledgments

This work was partially supported by the Japan Science and Technology Agency (JST) under Industry–Academia Collaborative R&D Program "Heterogeneous Structure Control: Towards Innovative Development of Metallic Structural Materials".

REFERENCES

1) Japan Society for Technology of Plasticity: *Fundamentals of Titanium and Its Working*, (Corona Publishing Co., Ltd., 2008).
2) M. Niinomi: *Basic Materials Science, Manufacturing and Newly Advanced Technologies of Titanium and Its Alloys*, (CMC Publishing Co., Ltd., 2009).
3) K. Wang: Mater. Sci. Eng. A **213** (1996) 134–137.
4) M. Niinomi, M. Nakai and J. Hieda: Acta Biomater. **8** (2012) 3888–3903.
5) M.T. Mohammed: Karbala Int. J. Mod. Sci. **3** (2017) 224–230.
6) I. Ohkata: J. Jpn. Soc. Mech. Eng. **107** (2004) 532–535.
7) S. Georgiadis, A.J. Gunnion, R.S. Thomson and B.K. Cartwright: Compos. Struct. **86** (2008) 258–268.
8) M. Balazic, J. Kopac, M.J. Jackson and W. Ahmed: Int. J. Nano Biomater. **1** (2007) 3–34.
9) S. Li, B. Sun, H. Imai, T. Mimoto and K. Kondoh: Compos., Part A **48** (2013) 57–66.
10) X. Zhang, F. Song, Z. Wei, W. Yang and Z. Dai: Sci. Eng. A **705** (2017) 153–159.
11) M.J. Bermingham, S.D. McDonald, M.S. Dargusch and D.H. StJohn: Scr. Mater. **58** (2008) 1050–1053.
12) S. Mereddy, M.J. Bermingham, D.H. StJohn and M.S. Dargusch: J. Alloys Compd. **695** (2017) 2097–2103.
13) Y. Murayama, M. Mikami, S. Ishiyama and S. Hanada: J. Jpn. Inst. Met. **57** (1993) 628–636.
14) B. Sun, S. Li, H. Imai, T. Mimoto, J. Umeda and K. Kondoh: Mater. Sci. Eng. A **563** (2013) 95–100.
15) D. Kang, K. Lee, E. Kwon and T. Tsuchiyama: Mater. Sci. Eng. A **632** (2015) 120–126.
16) Y. Yamabe, J. Umeda, H. Imai and K. Kondoh: J. Jpn. Soc. Powder Powder Metallurgy **64** (2017) 275–280.
17) H. Conrad: Prog. Mater. Sci. **26** (1981) 123–403.
18) L.C. Tsao: Mater. Sci. Eng. A **689** (2017) 203–211.
19) J. Greggi and W.A. Soffa: Scr. Metall. **14** (1980) 649–652.
20) Y. Kobayashi, Y. Tanaka, K. Matsuoka, K. Kinoshita, Y. Miyamoto and H. Murata: J. Soc. Mater. Sci., Japan **54** (2005) 66–72.
21) P. Luo, D.T. McDonald, W. Xu, S. Palanisamy, M.S. Dargusch and K. Xia: Scr. Mater. **66** (2012) 785–788.
22) A.H. Cottrell, S.C. Hunter and F.R.N. Nabarro: Philos. Mag. **44** (1953) 1064.
23) R.L. Fleischer: Acta Metall. **11** (1963) 203–209.
24) J. Friedel: *Dislocations*, (Pergamon Press, New York, 1964).
25) N.F. Motto and F.R.N. Nabarro: *Strength of Solids*, (Physical Society, London, 1947).
26) R. Labusch: Phys. Status Solidi **41** (1970) 659–669.
27) W.L. Finley and J.A. Snyder: Trans. AIME, **188** (1950) 277–285.
28) F. Watari and F. Nishimura: Journal of the Japanese Society for Dental Materials and Devices **10** (1991) 266–274.
29) S.A. Souza, C.R.M. Afonso, P.L. Ferrandini, A.A. Coelho and R. Caram: Mater. Sci. Eng. C **29** (2009) 1023–1028.
30) L. Bäcke: ISIJ Int. **50** (2010) 239–247.
31) M. Suehiro: ISIJ Int. **38** (1998) 547–552.
32) R.L. Gall and J.J. Jonas: Acta Mater. **47** (1999) 4365–4374.
33) C. Cai, S. LingHui, D. XingHao and W. BaoLin: Mater. Charact. **131** (2017) 72–77.
34) Y. Mikami, K. Oda, M. Kamaya and M. Mochizuki: Mater. Sci. Eng. A **647** (2015) 256–264.
35) K. An, L. Yuan, L. Dial, I. Spinelli, A.D. Stoica and Y. Gao: Mater. Des. **135** (2017) 122–132.
36) S. Kim, D. Kim, K. Lee, H. Cho and H.N. Han: Mater. Charact. **109** (2015) 88–94.
37) I.P. Jones and W.B. Hutchinson: Acta Metall. **29** (1981) 951–968.
38) C. Ikenmeyer and G. Panova: Adv. Math. **319** (2017) 40–66.